

Analyst

Accepted Manuscript



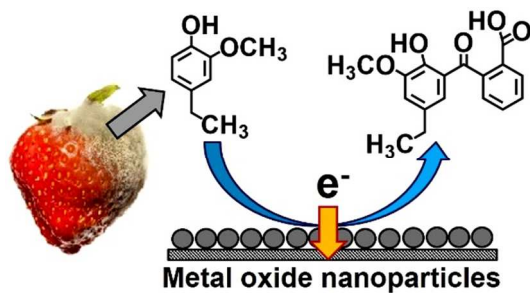
This is an *Accepted Manuscript*, which has been through the Royal Society of Chemistry peer review process and has been accepted for publication.

Accepted Manuscripts are published online shortly after acceptance, before technical editing, formatting and proof reading. Using this free service, authors can make their results available to the community, in citable form, before we publish the edited article. We will replace this *Accepted Manuscript* with the edited and formatted *Advance Article* as soon as it is available.

You can find more information about *Accepted Manuscripts* in the [Information for Authors](#).

Please note that technical editing may introduce minor changes to the text and/or graphics, which may alter content. The journal's standard [Terms & Conditions](#) and the [Ethical guidelines](#) still apply. In no event shall the Royal Society of Chemistry be held responsible for any errors or omissions in this *Accepted Manuscript* or any consequences arising from the use of any information it contains.

Table of Content Figure



High sensitive detection of *p*-ethylguaiacol at low concentrations using SnO_2 and TiO_2 metal oxide nanoparticles.

Cite this: DOI: 10.1039/c0xx00000x

www.rsc.org/xxxxxx

ARTICLE TYPE

Electrochemical detection of *p*-ethylguaiaicol, a fungi infected fruit volatile using metal oxide nanoparticles

Yi Fang, Yogeswaran Umasankar, Ramaraja P. Ramasamy*

Received (in XXX, XXX) Xth XXXXXXXXX 20XX, Accepted Xth XXXXXXXXX 20XX

DOI: 10.1039/b000000x

Nanoparticles of TiO₂ or SnO₂ on screen printed carbon electrode (SP) have been developed for evaluating their potential application in electrochemical sensing of fruits and plants volatiles. These metal oxide nanoparticle modified electrodes possess high sensitivity and low detection limit for the detection of *p*-ethylguaiaicol, a fingerprint compound present in the volatile signature of fruits and plants infected with a pathogenic fungus *Phytophthora cactorum*. The electroanalytical data obtained using cyclic voltammetry and differential pulse voltammetry showed that both SnO₂ and TiO₂ exhibited high sensitivity (174 to 188 for $\mu\text{m cm}^{-2}$) and low limit of detection limits (35 to 62 nM) for *p*-ethylguaiaicol detection. The amperometric detection was highly repeatable with RSD values ranging from 2.48 to 4.85%. The interference studies show that the other common plant volatiles do not interfere in the amperometric detection signal of *p*-ethylguaiaicol. The results demonstrate that metal oxides are reasonable alternative to expensive electrode materials such as gold or platinum for amperometric sensor applications.

Keywords: *Phytophthora cactorum*, *p*-ethylguaiaicol, tin oxide, titanium oxide, plant volatile sensor.

1. Introduction

The leather rot also called crown rot, is a plant disease caused by a pathogenic fungus *Phytophthora cactorum* which is known to infect a variety of cucurbit crops in southeastern United States.¹ As high as 50% of the 1.3 million tons of strawberries produced in the U.S. are affected by this disease and cause massive agro-economical loss every year.² There is an ever-increasing need for advanced detection and prevention of this disease to improve agricultural productivity. Plants produce unique volatile signature when infected by pathogens.^{3,4} Detecting these volatiles could help confirm the occurrence or existence of pathogen infection in agricultural crops. Attempts have been made previously to develop electronic nose for plant volatile profiling.⁵ Unlike GC-MS or GC/FID, which involves time consuming multiple stages of expert analysis, electronic nose refers to sensor arrays capable of reproducing human senses and pattern recognition systems. Since 1982 electronic noses have evolved to a practical device which could detect and recognize odors and flavors.⁶ Since its development, electronic noses have been applied to different areas from poultry, environment protection, food safety and medical care. It has been applied also for organic volatile compounds study.⁷⁻⁹ The distinctive symptom of leather rot in strawberries is the unpleasant odor produced by volatile compounds. One such symbolic volatile compound produced during *P. cactorum* infection is *p*-ethylguaiaicol.¹ Therefore detecting the production of

p-ethylguaiaicol by strawberry plants will be a useful indicator for the confirmation of the leather rot disease. However in order to detect at an early stage, the detection technology must be able to detect the compound at ultra-low concentrations. A variety of methods have been established for *p*-ethylguaiaicol detection over the years, including gas chromatography-mass spectroscopy (GC-MS), headspace-solid-phase microextraction-gas chromatography and HPLC-DAD-Fluorescence.¹⁰⁻¹³ However, all these methods require detailed sampling and cannot be used for real-time or non-destructive analysis.

Electrochemical sensing is a popular technology for non-destructive, real time detection of target analytes. Amperometric electrochemical sensors possess high sensitivity, high accuracy, high selectivity (when modified with a biomarker), enable rapid detection and are suitable for field application.¹⁴ Although enzymatic biosensors usually demonstrate high selectivity, non-enzymatic biosensors have also been developed and demonstrated before.^{15,16} We have previously demonstrated selective amperometric detection of plant volatile compounds on electroactive gold transducers.^{17,18} As conceptually shown in Figure 1, the *p*-ethylguaiaicol can be detected on the working electrode in an electrochemical cell based on the electrical signal generated during the oxidation of *p*-ethylguaiaicol on the surface of the electrode. The working electrode surface is modified with specific functional element that also acts as transducer transmitting the electrical signal from the surface. While gold

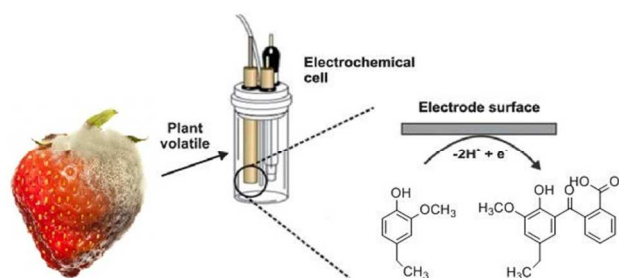


Fig. 1 Schematic of the electrochemical cell containing metal oxide modified electrode for the detection of *p*-ethylguaiaicol which was released from *Phytophthora cactorum* infection.

nanoparticles and carbon nanotubes have been widely explored as electrochemical transducers for amperometric sensors, metal oxides have not been explored in great detail for this application. The rationale for adopting metal oxide nanoparticles in this work was due to their advantages compared to commonly used nanomaterials. The advantages are (1) metal oxide nanoparticles are catalyst for the dehydrogenation of alcoholic compounds such as aliphatic alcohols, acetic acid etc., which could enhance the plant volatile reaction on the transducer,¹⁹ (2) metal oxides are inexpensive compared to noble metal nanoparticles,²⁰ (3) some metal oxides have large band gap (greater than 3.3 eV) which can enable them for amperometric signal generation in aqueous solution, (4) the preparation method for obtaining required size and shape of these nanoparticles are easier compared to other nanostructure synthesis. In this work, we used two metal oxides – SnO₂ and TiO₂ as electrochemical detection elements for amperometric sensing. Screen-printed carbon (SP) electrodes were modified with nanoparticles of SnO₂ or TiO₂ and used for the electrochemical detection of *p*-ethylguaiaicol in simulated fruit volatile samples.

2. Experimental

2.1. Materials

Tin (IV) oxide (<100 nm) and titanium (IV) oxide (~21 nm) nanoparticles obtained from Sigma-Aldrich were used for preparing nanoparticle suspensions. *p*-ethylguaiaicol from Frinton Laboratories, Inc., (New Jersey, US) was used as received. *p*-ethylphenol was purchased from Sigma-Aldrich and used for interference and synthetic real sample studies. *cis*-3-hexenol, hexyl acetate, *cis*-hexen-1-yl acetate, 1-octen-3-ol and 3-octanone obtained from TCI America (Portland, OR) were used as received. All other chemicals used were of analytical grade. All aqueous solutions were prepared using 18.2 MΩ nanopure de-ionized (DI) water. 0.1M electrolyte solution of potassium hydrogen phthalate (KHP) (pH 4) was prepared for all the experiments. Solutions were deoxygenated by purging with pre-purified nitrogen gas for 15 min before each electrochemical measurement.

2.2. Apparatus

Cyclic voltammetry and differential pulse voltammetry were performed using CHI model 920c potentiostat. For electrochemical measurements a conventional three-electrode cell assembly consisting of a 3M Ag/AgCl reference electrode and a

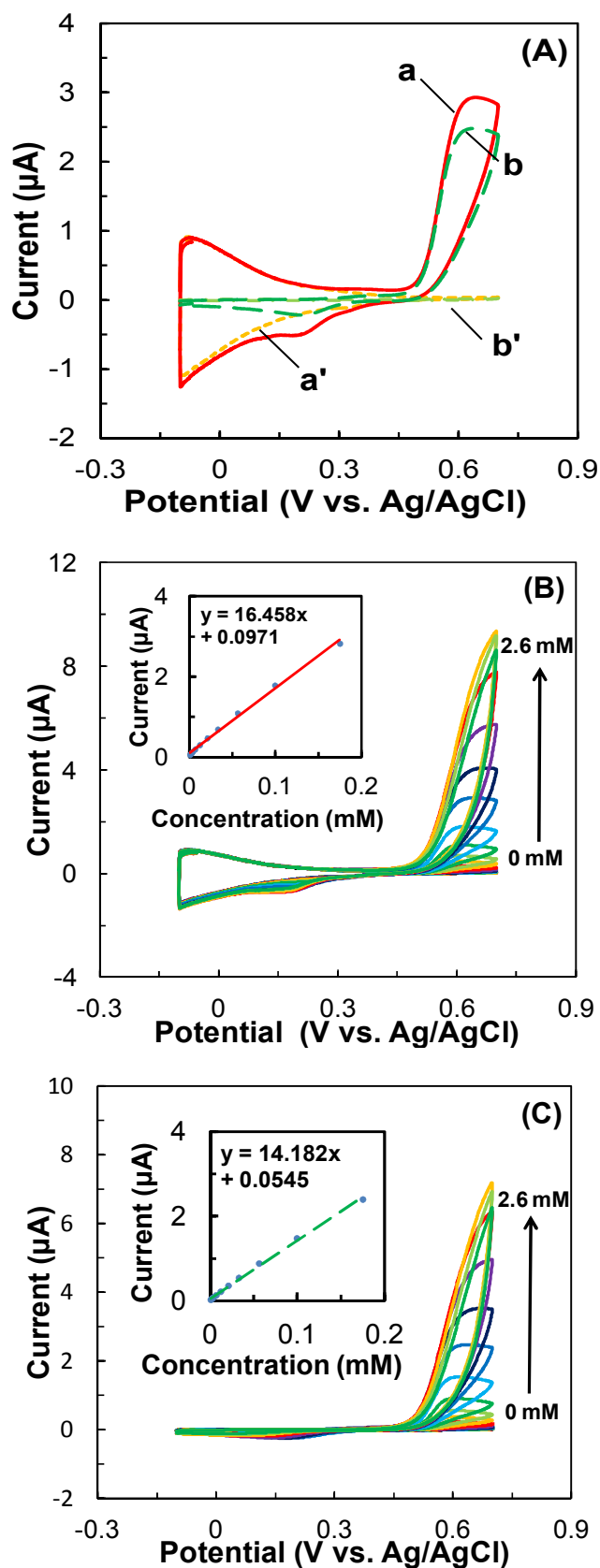


Fig. 2 CV responses of SnO₂-SP (a and a') and TiO₂-SP (b and b') with (a and b) and without (a' and b') the presence of 0.17 mM *p*-ethylguaiaicol (A); Concentration effect of *p*-ethylguaiaicol at SnO₂-SP (B) and TiO₂-SP (C) electrodes.

Table 1 Comparison of sensitivity, linear range, LOD and LOQ of *p*-ethylguaiaicol at different electrodes obtained using different electrochemical techniques.

Electrode	pH	Technique	E_{pa} (V)	Linear range (R^2)	Sensitivity ($\mu\text{A cm}^{-2} \text{mM}^{-1}$)	LOD(nM)	LOQ(nM)
SnO ₂ -SP	4	CV	0.62	0.6 μM -0.17mM (0.9954)	232	82	249
		DPV	0.54	0.2 μM -0.1mM (0.9932)	174	62	188
TiO ₂ -SP	4	CV	0.62	0.6 μM -0.17mM (0.9972)	200	126	382
		DPV	0.54	0.2 μM -0.1mM (0.9934)	188	35	106

Pt wire counter electrode was used for electrochemical measurements. All potentials are reported with respect to 3M Ag/AgCl reference electrode. The working electrode was a screen-printed carbon electrode (SP) modified either with SnO₂ nanoparticles or TiO₂ nanoparticles. All experiments were carried out at 25 °C ± 2.

2.3. Electrode preparation

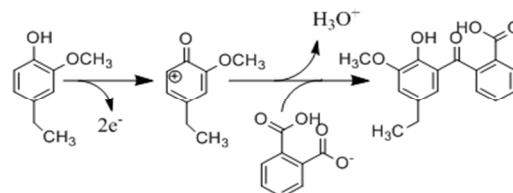
SnO₂ and TiO₂ nanoparticle suspensions were prepared by ultrasonication of 1 mg of the respective nanoparticles in 1 mL DI water. The SnO₂ and TiO₂ nanoparticle modified SP electrodes were prepared by drop casting 18 μL (in three steps of 6 μL additions) of the nanoparticle suspension on the SP, followed by drying at 70 °C. The cyclic voltammogram (CV) and differential pulse voltammogram (DPV) studies were done in a 10 mL voltammetry cell containing N₂ saturated 0.1M potassium hydrogen phthalate (KHP) electrolyte for SnO₂ as well as TiO₂. The potential range scanned for CV studies were for metal oxide modified SP electrodes at the scan rate of 0.02 Vs⁻¹. For DPV the potential scanned was from -0.1 to 0.7 V with the increment of 0.004 V, amplitude 0.05 V, pulse width 0.2 s and pulse period 0.5 s for all electrodes.

3. Results and discussion

3.1. Electrochemical response of *p*-ethylguaiaicol on metal oxide modified SPs

The metal oxide modified electrodes were characterized using cyclic voltammetry in the presence and absence of *p*-ethylguaiaicol. Although acidic conditions favor *p*-ethylguaiaicol oxidation as found in our experiments (data not shown), a pH 4 KHP electrolyte was used in our studies to avoid reaction between metal oxides and electrolyte. The cyclic voltammograms of SnO₂ and TiO₂ modified electrodes in the presence and absence of *p*-ethylguaiaicol are shown in Figure 2a and the results († supplementary data Fig. S1a) demonstrate the better sensitivity of *p*-ethylguaiaicol detection by metal oxide nanoparticle modified electrodes when compared with unmodified screen printed (SP) carbon electrode. In the absence of *p*-ethylguaiaicol, TiO₂ showed no redox activity, and SnO₂ exhibited broad redox peaks in the potential window of -0.1 to 0.4 V, which correspond to the adsorption and desorption of phthalate ions, a known

behavior for SnO₂ in KHP electrolyte.^{21,22} In the presence of *p*-ethylguaiaicol, both metal oxides exhibited irreversible peaks at 0.62 V (oxidation) and at 0.2 V (reduction). The irreversible oxidation of *p*-ethylguaiaicol at 0.62V, occurs as per equation 1, where *p*-ethylguaiaicol forms phenoxy radical intermediate, which then reacts with phthalate anion in the electrolyte to form benzoic acid derivative and H₃O⁺ (second step in equation 1).^{23,24} The irreversible reduction peak in the cyclic voltammograms at 0.2 V could be due to the reduction of phenoxy radical to *p*-ethylguaiaicol. The result suggests that at potentials below 0.2 V, the *p*-ethylguaiaicol oxidation is reversible.



→ [1]

Comparison of *p*-ethylguaiaicol oxidation peaks (at 0.62 V) shows both SnO₂ and TiO₂ possess similar oxidation currents. The effect of *p*-ethylguaiaicol concentration on the oxidation currents was studied and reported in Figure 2b and c SnO₂ and TiO₂ respectively. The stepwise increase in *p*-ethylguaiaicol concentration from 0.2 μM to 2.6 mM in the electrochemical cell was achieved by adding *p*-ethylguaiaicol from the series of standard concentrations. The above concentration range was chosen by a series of experiments, where the lowest limit was determined based on the noticeable increase in oxidation current upon an incremental addition of *p*-ethylguaiaicol into the electrolyte. Similarly, the upper concentration limit was chosen based on the rate of decrease in oxidation current during subsequent additions of *p*-ethylguaiaicol. The cyclic voltammetry results in Figure 2b and c show that increasing concentration of *p*-ethylguaiaicol increased the oxidation peak current (I_{pa}) of *p*-ethylguaiaicol oxidation on both SnO₂ and TiO₂ electrodes. The initial response to *p*-ethylguaiaicol additions showed a shift in the *p*-ethylguaiaicol oxidation peak potential (E_{pa}) from 0.62 V to 0.7 V. This could be attributed to the increase in acidity of the electrolyte due to more H₃O⁺ formation (refer equation 1).

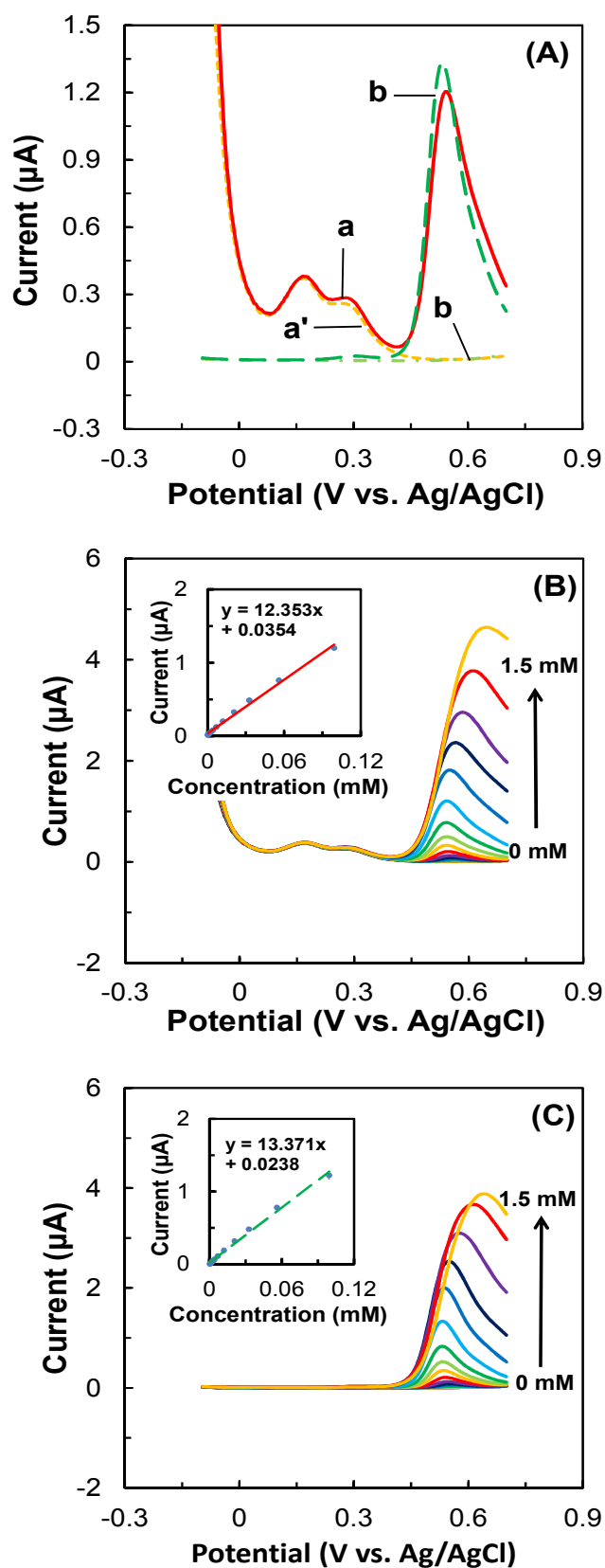


Fig. 3 DPV responses of SnO₂-SP (a and a') and TiO₂-SP (b and b') with (a and b) and without (a' and b') the presence of 0.17 mM *p*-ethylguaiacol (A); Concentration effect of *p*-ethylguaiacol on SnO₂-SP (B) and TiO₂-SP (C) electrodes.

The electroanalytical data such as sensitivity, limit of detection (LOD) at the signal to noise ratio of 3, and limit of quantification (LOQ) of both SnO₂ and TiO₂ electrodes derived using equation 2, 3 and 4 and are listed in Table 1 respectively.

$$\text{Sensitivity} = \frac{\text{Slope of calibration curve } (A M^{-1})}{\text{Area of electrode } (cm^2)} \rightarrow [2]$$

$$\text{LOD} = 3 \times \frac{\text{Standard deviation of peak current in the absence of analyte}}{\text{Slope of linear calibration curve } (A M^{-1})} \rightarrow [3]$$

$$\text{LOQ} = 10 \times \frac{\text{Standard deviation of peak current in the absence of analyte}}{\text{Slope of linear calibration curve } (A M^{-1})} \rightarrow [4]$$

Comparison of sensitivity values obtained through cyclic voltammogram given in Table 1 reveals that SnO₂ had higher sensitivity, lower LOD and LOQ than TiO₂ although the difference was not significant. Though CV provides a firsthand understanding of the electrochemistry of the system, biosensor applications demand chronoamperometric or pulse methods to eliminate the noise caused by the capacitance and resistance in order to improve overall electroanalytical measurement accuracy.²⁵

Therefore, differential pulse voltammetry (DPV) was used in a similar manner to CV to study *p*-ethylguaiacol oxidation between -0.1 and 0.7 V. Compared to unmodified SP electrode, TiO₂ and SnO₂ modified electrodes display higher sensitivity for *p*-ethylguaiacol detection († supplementary data Fig. S1b). Similar to CV results, DPV also showed peaks in the absence of *p*-ethylguaiacol on SnO₂, due to the adsorption and desorption of phthalate ions. In the presence of *p*-ethylguaiacol, the oxidation peaks appeared at 0.54 V (E_{pa}) with similar I_{pa} values for both the electrodes as shown in Figure 3a. The *p*-ethylguaiacol characteristic peaks for both SnO₂ and TiO₂ were similar to that of cyclic voltammograms with ~0.05 V negative shift due to the applied amplitude (0.05 V) during DPV measurements. The peaks currents (I_{pa}) for *p*-ethylguaiacol oxidation increased with the concentration in the range of 0.2 µM to 1.5 mM on both electrodes as shown in Figure 3b and c. The inset figures show a linear dependency of I_{pa} on concentration. The empirical electroanalytical values derived from the DPV data are also given in Table 1. Due to the elimination of capacitance as well as adsorption-desorption effects in DPV († supplementary data Fig. S2), the values for DPV showed lower sensitivity, but better detection and quantification limits for both electrodes when compared to their corresponding CV values. However TiO₂ exhibited better sensitivity and detection limits than SnO₂ according to the DPV results, although the difference is not significant (Table 1). DPV values are better representative of the sensing characteristic of the electrodes due to the elimination of parasitic currents from the true oxidation response of *p*-ethylguaiacol. The results suggest that both SnO₂ and TiO₂ could be used to construct amperometric sensors for *p*-ethylguaiacol detection at concentrations relevant to typical infected fruit volatiles.

3.2. Reproducibility and re-usability studies

Eight SnO₂ and TiO₂ modified SP electrodes were prepared under similar conditions and tested for *p*-ethylguaiacol oxidation using DPV. The DPV peak currents (I_{pa}) at 0.54 V, for all eight electrodes were measured at concentration of 2.5 mM. The high

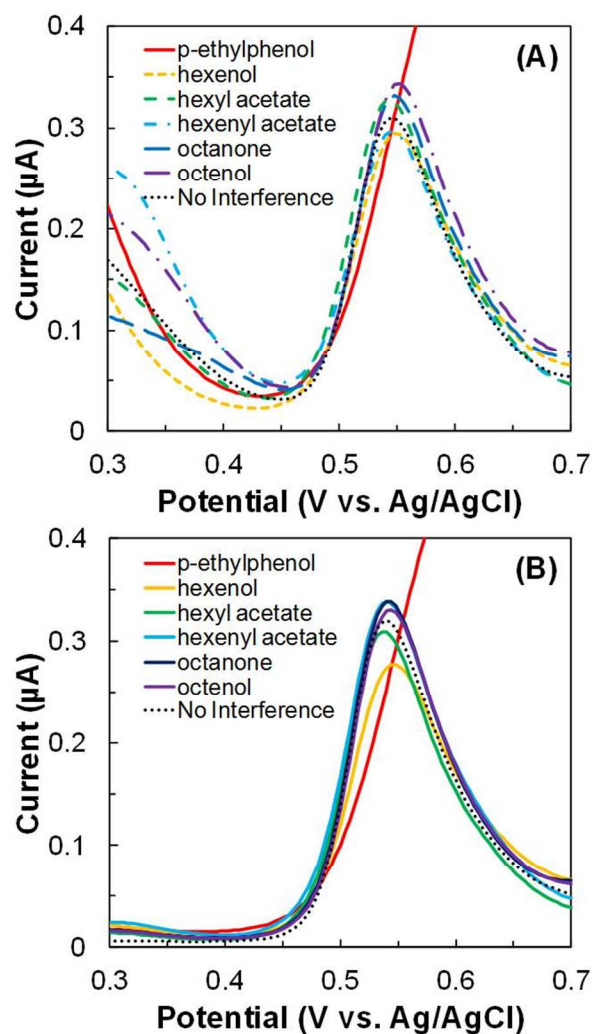


Fig 4 Interference study of 20.8 μM *p*-ethylguaiaicol with 6 different compounds *p*-ethylphenol, *cis*-3-hexen-1-ol, hexyl acetate and *cis*-3-hexen-1-yl acetate, 3-octanone and 1-octen-3-ol on $\text{SnO}_2\text{-SP}$ (A) and $\text{TiO}_2\text{-SP}$ (B) by DPV.

concentration was chosen to ensure that even subtle changes in measured currents can be determined. The results († supplementary data Table S1) showed that the peak current for all eight electrodes varied within 2.48 and 4.85 % for SnO_2 and TiO_2 respectively. The low variability indicates high reproducibility of the observed results for both electrodes.

The reusability or stability of SnO_2 and TiO_2 modified SP electrodes were tested in a series of DPV experiments at 2.5 mM *p*-ethylguaiaicol concentration on consecutive days for a period of 15 days. I_{pa} of *p*-ethylguaiaicol oxidation in DPVs was measured on each day and percentage decrease in current decrease over time was calculated from the measurements († supplementary data Table S2). The results showed a loss of activity up to 67 % for SnO_2 and 81 % for TiO_2 after 15 days. Though the currents decreased significantly over time, the rate of decrease slowed down after the first two days with no large decrease beyond the first week. The loss in stability could be attributed to the formation of surface oxides and other adsorption effects from the ions present in the electrolyte that tend to slowly poison the electrode over the long-term.

3.3. Interference of other plant volatiles in *p*-ethylguaiaicol determination

The infected plant volatile contains other chemical compounds that are non-specific to the infection and often released at much higher concentrations than *p*-ethylguaiaicol. A representative set of such compounds was selected and their interference effects on *p*-ethylguaiaicol measurements were studied using DPV. The compounds used to study interference were *p*-ethylphenol, 3-octanone, 1-octen-3-ol, *cis*-3-hexenol, hexyl acetate and *cis*-hexen-1-yl acetate. *p*-ethylphenol, 3-octanone and 1-octen-3-ol are present in the chemical signature of the *Phytophthora cactorum* itself.¹ The other three compounds *cis*-3-hexenol, hexyl acetate and *cis*-hexen-1-yl acetate are green leaf volatiles that are common to most plants.¹⁸ The fungi infected plant typically release 0.2 μM of 3-octanone, 0.2 μM of 1-octen-3-ol, 10 μM of *cis*-3-hexenol, 1.2 μM of hexyl acetate and 20 μM of *cis*-hexen-1-yl acetate.^{18,26} Therefore these concentrations were used in our interference study. The experiments were conducted separately for each of the six interfering compounds where the *p*-ethylguaiaicol concentration was kept constant and as low as possible (20.8 μM), but within the linear response (I_{pa}) region obtained in DPV. The results showed characteristic peaks for *p*-ethylguaiaicol even in the presence of interfering compounds as shown in Figures 4a and b for SnO_2 and TiO_2 respectively. On both SnO_2 and TiO_2 electrodes, the addition of *p*-ethylphenol significantly changed the DPV wave above 0.55 V but not at the peak oxidation potential (0.54 V) of *p*-ethylguaiaicol (Figure 4a and b). As shown by the calculated I_{pa} values in Table 2, *p*-ethylphenol interference was limited to ± 6.7 % for SnO_2 and TiO_2 respectively. Addition of *cis*-hexen-1-yl acetate showed less than 2 % interference on *p*-ethylguaiaicol signal on TiO_2 , but up to 12 % interference on SnO_2 . The reason for this difference is not clearly understood. Other compounds such as 3-octanone or 1-octen-3-ol or *cis*-3-hexenol or hexyl acetate did not show any significant interference on the *p*-ethylguaiaicol signal and the interference was limited to less than 2 %. The studies above indicate *p*-ethylguaiaicol detection on metal oxide modified electrodes does not suffer any significant interference from both fungal and green leaf volatile compounds.

3.4. *p*-ethylguaiaicol determination in simulated fruit volatile

The ability of SnO_2 or TiO_2 for the determination of *p*-ethylguaiaicol in real infected samples was evaluated using simulated chemical mixture that mimics the composition of the real fruit volatile signature. As discussed in the previous section, chemical signature from infected plants will contain both the green leaf volatiles and the volatiles from the pathogen itself. Two sets of samples were used for simulation: (i) only infected fruit volatiles and (ii) both infected fruit and green leaf plant volatiles. The composition of (i) was 20.8 mM *p*-ethylguaiaicol, 2.5 mM *p*-ethylphenol, 2.5 μM 3-octanone and 2.5 μM 1-octen-3-ol. The composition of (ii) includes all (i) in addition to 10 μM *cis*-3-hexen-1-ol, 1.25 μM hexyl acetate and 25 μM *cis*-hexen-1-yl acetate. The above concentrations were chosen based on the composition of typical chemical signature of *Phytophthora cactorum* infection.^{1,26} The experiments were done using DPV and the *p*-ethylguaiaicol oxidation current was measured for detailed analysis. Parameters such as the concentrations added in

Table 2 Interference study of 20.8 μ M *p*-ethylguaicol with 6 different compounds *p*-ethylphenol, *cis*-3-hexen-1-ol, hexyl acetate and *cis*-3-hexen-1-yl acetate, 3-octanone and 1-octen-3-ol by DPV

Electrode	Compound	Concentration	Current (μ A)	Activity (%)
SnO ₂ -SP	<i>p</i> -ethylphenol	0	0.3212	100
		2.50mM	0.3533	110.01
	<i>cis</i> -3-hexen-1-ol	0	0.2906	100
		32 μ M	0.2956	101.73
	hexyl acetate	0	0.3249	100
		2 μ M	0.3274	100.76
	<i>cis</i> -3-hexen-1-yl acetate	0	0.2672	100
		32 μ M	0.2972	111.21
	3-octanone	0	0.3301	100
		2 μ M	0.3320	100.57
	1-octen-3-ol	0	0.3381	100
		2 μ M	0.3436	101.62
TiO ₂ -SP	<i>p</i> -ethylphenol	0	0.3459	100
		2.50mM	0.3227	93.3
	<i>cis</i> -3-hexen-1-ol	0	0.2783	100
		32 μ M	0.2782	99.96
	hexyl acetate	0	0.3060	100
		2 μ M	0.3092	101.08
	<i>cis</i> -3-hexen-1-yl acetate	0	0.3336	100
		32 μ M	0.3400	101.91
	3-octanone	0	0.3334	100
		2 μ M	0.3391	101.70
	1-octen-3-ol	0	0.3278	100
		2 μ M	0.3308	100.90

Table 3 Simulated sample study using typical chemicals released during *Phytophthora cactorum* infection of plants

Electrode	Sample	Added (μ A)	Found (μ A)	Recovery (%)	RSD (%)	
SnO ₂ -SP	Infected fruit	0.0455	0.0417	91.65	3.65	
		0.1942	0.1947	100.26		
		0.4816	0.4789	99.44		
	Infected fruit with plant	1.5130	1.5110	99.87	3.88	
		0.0455	0.0495	108.79		
		0.1942	0.2011	103.55		
	TiO ₂ -SP	Infected fruit	0.4816	0.4816	100.00	4.85
			1.5130	1.4890	98.41	
			0.0421	0.0389	92.40	
Infected fruit with plant		0.2218	0.2019	91.03	3.67	
		0.5017	0.5021	100.08		
		1.6210	1.6500	101.79		
Infected fruit with plant		0.0421	0.0399	94.77	3.67	
		0.2218	0.2070	93.33		
		0.5017	0.5067	101.00		
		1.6210	1.6420	101.30		

the experiment, found and relative standard deviation (RSD) obtained from the experiments were calculated from the DPV measurements and are listed in Table 3. The values show that the recovery of *p*-ethylguaicol in both simulated samples varied from 91 to 101% for both electrodes with RSD values between 4 and 5%. The analysis shows that both SnO₂ and TiO₂ electrodes can be used for *p*-ethylguaicol determination.

4. Conclusions

Both SnO₂ and TiO₂ have been demonstrated to show similar detection capabilities for *p*-ethylguaicol based on amperometric determination. Ultra low limits of detection were achieved by both metal oxide electrodes in DPV measurement. Both electrodes exhibited good reproducibility towards *p*-ethylguaicol determination. The CV and DPV data along with the chemical reactions established here elucidate the electrochemical reaction mechanisms pertaining to the amperometric sensing of *p*-

ethylguaiaicol. The electroanalytical data presented in this article can be used for both qualitative and quantitative determination of *p*-ethylguaiaicol. The synthetic sample studies presented in this work illustrate the approach for the development of *p*-ethylguaiaicol sensing during initial stages of *Phytophthora cactorum* infection.

Acknowledgement

We acknowledge the National Science Foundation (CBET-1159540) and ACS Herman Frasch Foundation (Grant # 045097-01) for financial support.

Notes and references

*Address, Nano Electrochemistry Laboratory, College of Engineering, University of Georgia, Athens, GA 30602, United States. Fax: +1-706-542-3804; E-mail: rama@uga.edu

† Electronic Supplementary Information (ESI) available:

1. H. Jeleń, J. Krawczyk, T. Larsen, A. Jarosz and B. Golebniak, *Lett Appl Microbil.*, 2005, **40**, 255.
2. M.A. Ellis and G. G. Grove, *Plant Dis.*, 1983, **67**, 549.
3. I. T. Baldwin, A. Kessler and R. Halitschke, *Curr Opin Plant Biol.*, 2002, **5**, 351.
4. P. W. Paré and J.H. Tumlinson, *Plant Pysiol.*, 1999, **121**, 325.
5. J. Laothawornkitkul, J. P. Moore, J. E. Taylor, M. Possell, T. D. Gibson, C. N. Hewitt and N. D. Paul, *Environ Sci Technol.*, 2008, **42**, 8433.
6. K. Persaud. and G. Dodd, *Nature.*, 1982, **299**, 352.
7. C. D. Natale, D. Salimbeni, R. Paolesse and A. Macagnano, A. D'Amico, *Sensor Actuat B-Chem.*, 2000, **65**, 220.
8. A. Z. Berna, J. Lammertyn, S. Saevels, C. D. Natale and B. M. Nicolai, *Sensor Actuat B-Chem.*, 2004, **97**, 324.
9. S. Saevels, J. Lammertyn, A. Z. Berna, E. A. Veraverbeke, C. D. Natale and B. M. Nicolai, *Postharvest Biol Tec.*, 2004, **31**, 9.
10. A. P. Pollnitz, K. H. Pardon and M. A. Sefton, *J Chromatogr A.*, 2000, **874**, 101.
11. S. Rayne and N. J. Eggers, *J Environ Sci Heal B.*, 2007, **42**, 887.
12. N. Martorell, M. P. Martí, M. Mestres, O. Busto and J. Guasch, *J Chromatogr A.*, 2002, **975**, 349.
13. P. Caboni, G. Sarais, M. Cabras and A. Angioni, *J Agr Food Chem.*, 2007, **55**, 7288.
14. E. Bakker and Y. Qin, *Anal Chem.*, 2004, **76**, 3285.
15. P. V. Suneesh, K. Chandhini, T. Ramachandran, B. G. Nair, T. G. Sathesh Babu, *Biosens Bioelectron.*, 2013, **50**, 472.
16. Z. Zhuang, X. Su, H. Yuan, Q. Sun, D. Xiao and M. M. F. Choi, *Analyst.*, 2008, **133**, 126.
17. Y. Umasankar and R. P. Ramasamy, *Analyst*, 2013, **138**, 6623.
18. Y. Umasankar, G. C. Rains and R. P. Ramasamy, *Analyst*, 2012, **137**, 3138.
19. B. P. J. d. L. Costello, R. J. Ewen, P. R. H. Jones, N. M. Ratcliffe and R. K. M. Wat, *Sensors and Actuators B*, 1999, **61**, 199.
20. U. Diebold, *Appl Phys A-Mater.*, 2003, **76**, 681.
21. N. R. Armstrong, A. W. C. Lin, M. Fujihira and T. Kuwana, *Anal Chem*, 1976, **48**, 741.
22. P. Lian, X. Zhu, S. Liang, Z. Li, W. Yang and H. Wang, *Electrochimica Acta*, 2011, **56**, 4532.
23. A. Sadana and J. R. Katzer, *J Catal.*, 1974, **35**, 140.
24. C. Comminellis and C. Pulgarin, *J Appl Electrochem.*, 1993, **23**, 108.
25. S. P. Kounaves in *Handbook of Instrumental Techniques for analytical Chemistry*, ed. A. A. Settle, Prentice Hall PTR, Upper Saddle River, NJ, 1997, Ch 37, pp. 709-726.
26. A. Sunesson, W. Vaes, C. Nilsson, G. Blomquist, B. Andersson and R. Carlson, *Appl Environ Microb.*, 1995, **61**, 2911.